FLEXIBLE MICROCOILS FOR MAGNETIC RESONANCE IMAGING OF THE BILE DUCT

M.M.Ahmad[1], R.R.A.Syms[1*], I.R.Young[1], B. Matthew[1],
W.Casperz[2], S.Taylor-Robinson[3], W.Gedroyc[2]
[1]EEE Dept., Imperial College, Exhibition Road, London, SW7 2AZ, UK
[2]Dept. of Radiology and [3]Dept. of Medicine, St Mary's Hospital, Praed St., London, W2 1NY, UK
[*] **r.syms@ic.ac.uk**

Abstract *— Miniature flexible RF coils for magnetic resonance imaging have been constructed using electroplated conductors and substrates formed in SU-8 epoxy photoresist. The coils are batch fabricated on glass wafers, removed by thermal shock and integrated into a catheter probe designed for endoscopic insertion into the bile duct.* ^{1}H *MRI with at least 1 mm resolution is demonstrated in vitro using microfabricated phantoms and liver tissue at 1.5 T.*
Key Words: *Magnetic resonance imaging, Microcoil, MEMS*

I INTRODUCTION

Cholangiocarcinomas are malignant tumours of the lining of the bile duct [1]. They are insensitive to chemotherapy and radiotherapy, and only small (≈ 1 mm) tumours are operable. Imaging is performed during endoscopic retrograde cholangio-pancreatography using fluoroscopic X-ray screening and a side-viewing flexible endoscope [2]. Direct viewing of the duct is only possible near its distal end, although catheters can be inserted via a side-opening biopsy channel (Fig. 1). Histological confirmation involves sampling with a cytology brush [3]. This process retains some malignant cells, but can also seed them along the duct. Conventional magnetic resonance imaging (MRI) currently has too low resolution to detect operable tumours. Advantages would be obtained by performing MRI with internal coils, using a catheter probe with a cytology brush. Probes based on planar-loop, opposed-solenoid, meander and twisted-pair coils have been developed for vascular imaging and catheter tracking. Intrabiliary imaging has also been demonstrated with loopless catheter antennae [4]. Microfabricated coils have clear advantages in size and reproducibility, and have already been demonstrated on GaAs [5], Si [6], glass [7] and plastic [8]. Recently [9], we showed how planar fabrication may be used to form flexible resonant RF detectors combining thick electro-plated copper conductors with a substrate formed in the photopatternable epoxy SU-8 [10]. Here, we describe a prototype catheter detector based on a microfabricated coil (Fig. 2), and show how its performance may be quantified with micro-fabricated resolution test phantoms and tissue.

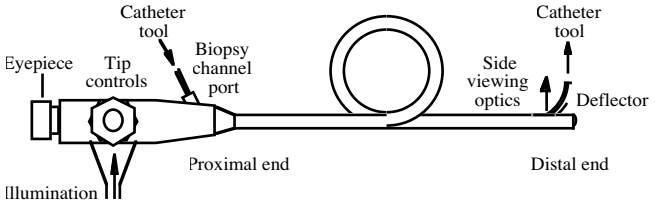

Figure 1.Side-opening endoscope.

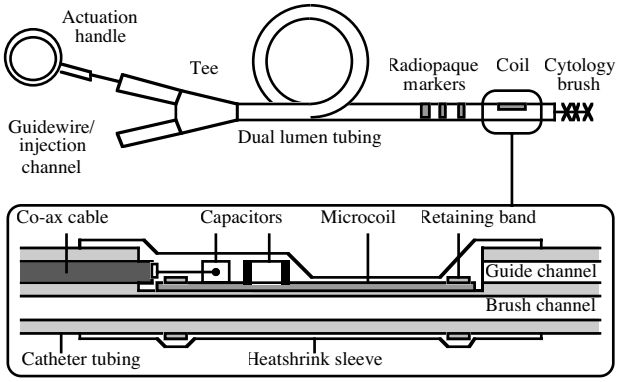

Figure 2. Modified cytology brush.

II COIL FABRICATION

Microcoils were fabricated as rectangular spirals with an inductor on one side of the substrate connected by vias to contact pads for capacitors for frequency tuning and impedance matching on the other (Fig. 3). To pass the biopsy channel (3.2 mm ID), the following design parameters were used: A = 2.7 mm, B = 25 mm, A_C = 2 mm, B_C = 10 mm, W = 200 μm and S = 100 μm. The highest performing coils were two-turn planar spirals. However, two-turn stacked spirals (which had windings on both sides of the plastic substrate (Fig. 4) were also fabricated, together with three-turn planar spirals and four-turn stacked spirals.

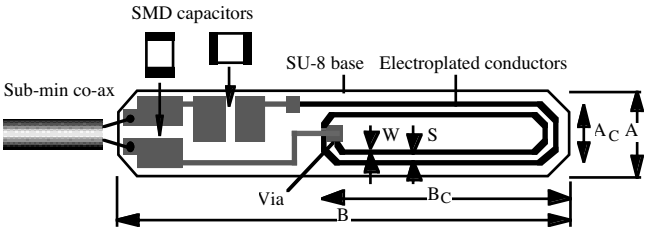

Figure 3. Layout of microcoil with 2-turn planar spiral.

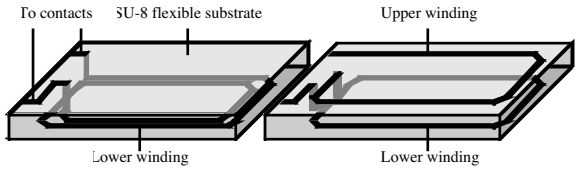

Figure 4. Comparison of planar and stacked windings.

Microcoils were fabricated as shown in Fig. 5. Here, a Pyrex glass wafer is used as a temporary carrier while electroplating of 12 μm Cu is carried out on either side of a 100 μm thick SU-8 interlayer. The parts are then detached by thermal shock to provide a set of flexible substrates carrying an embedded RF circuit. Fig. 6 shows a completed coil with a two-turn planar winding.

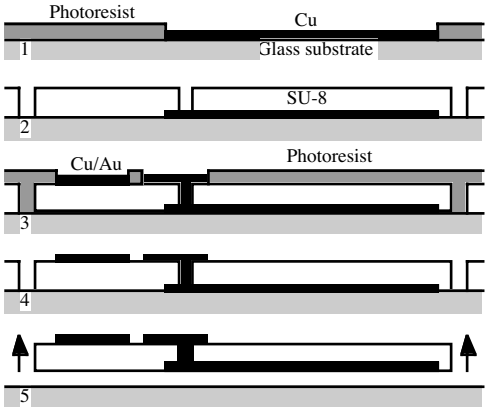

Figure 5. Fabrication process for flexible microcoils.

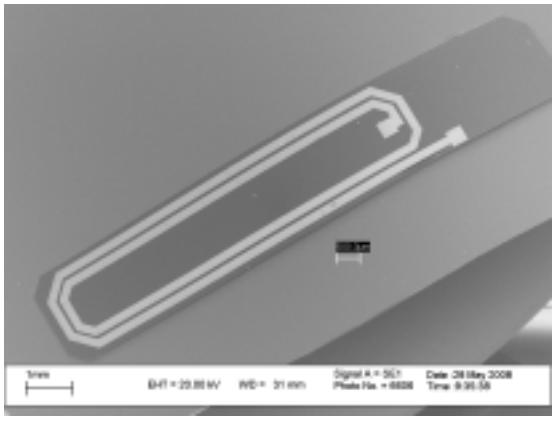

Figure 6. Completed microcoil.

III PHANTOM FABRICATION

Calibrated resolution test phantoms were also formed in SU-8. The phantoms consisted of periodic bar structures with a 1 : 1 mark-to-space ratio and linewidths of 1000 μm, 500 μm and 250 μm. When immersed in an organic liquid such as tetramethyl silane (TMS), such objects should appear opaque in MRI. Single-sided planar processing was again used for fabrication, this time using sacrificial silicon substrates as carrier wafers (Fig. 7). SU-8 was spin-coated over wafers that had been patterned and deep reactive ion etched to a depth of 250 μm. After exposure and development, the phantoms were detached by etching in KOH to leave stand-alone SU-8 parts (Fig. 8).

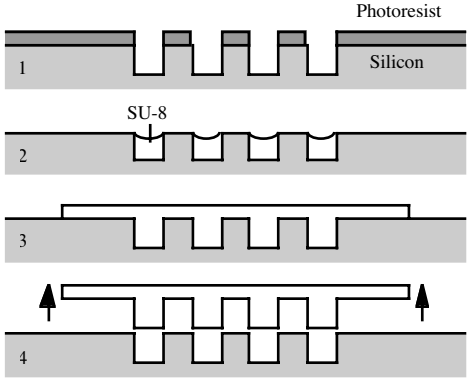

Figure 7. Fabrication process for resolution phantoms.

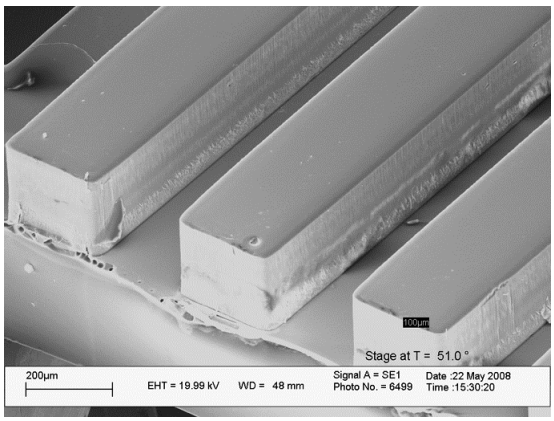

Figure 8. Microfabricated phantom.

IV MECHANICAL & ELECTRICAL TESTING

The mechanical behaviour of SU-8 was investigated by mounting short cantilevers on a piezoelectric stage driven by a signal generator, and determining the onset of mechanical resonance (Fig. 9). The Young's modulus (E) was then extracted from

standard formulae for the resonant frequency. Figure 10 shows the temperature dependence of E, which shows that major changes start occurring at ≈ 190 °C, close to the glass transition temperature (210 °C). Temperatures and times used for thermal shock detachment were therefore minimised.

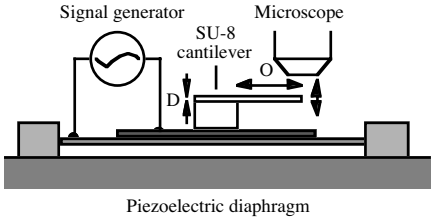

Figure 9. Arrangement for mechanical testing of SU-8.

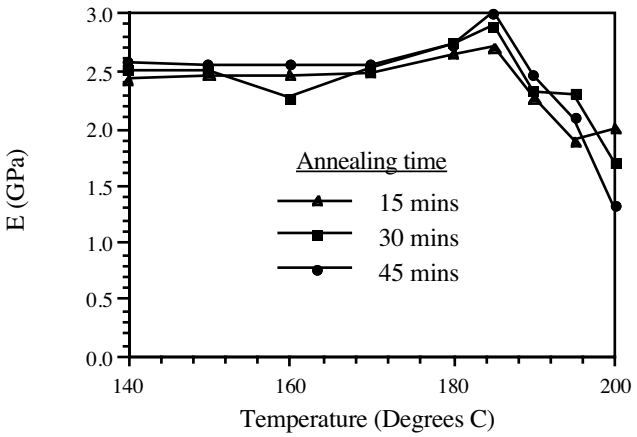

Figure 10. Variation of Young's Modulus of SU-8.

Electrical characterisation was performed using a network analyser. Two-turn coils with planar windings were selected as having the best overall performance, from the frequency dependence of the Q-factor (Fig. 11). Resonant detectors were then tuned and matched for 63.8 MHz (the operating frequency of ^{1}H MRI in a 1.5 T field) using additional non-magnetic capacitors (Fig. 12).

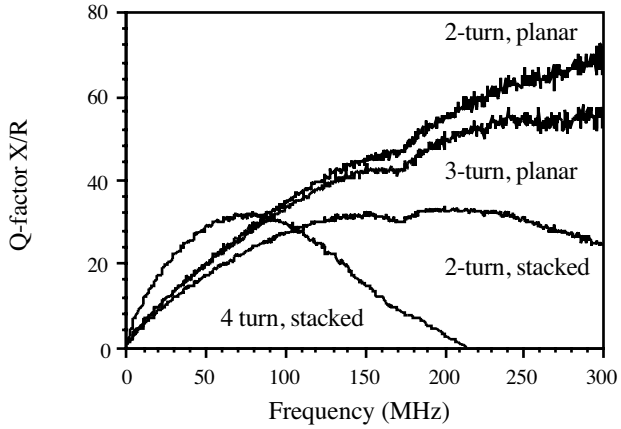

Figure 11. Q-factor variation of different coil types.

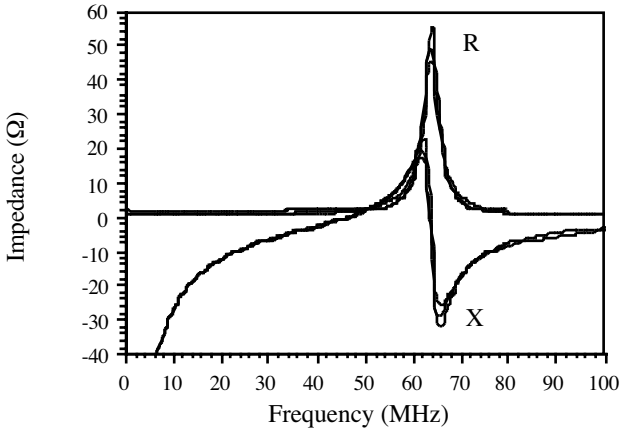

Figure 12. Impedance variation of 2-turn resonators.

V CATHETER INTEGRATION

Catheter probes were constructed by modifying a standard 8 Fr (2.7 mm dia) cytology brush unit (Cooks Cytomax II), removing all magnetic parts including the brush and excising a portion of one lumen to site the coil (Fig. 13). Electrical connection was made using 0.8 mm dia co-ax cable.

Figure 13. Tip of modified cytology brush unit.

VI MAGNETIC RESONANCE IMAGING

^{1}H MRI was performed using a 1.5 T GE HD Signa Excite scanner. The system body coil was used for transmission and the microcoil for signal reception. The microcoil was placed at the isocentre in the coronal plane. Fig. 14 shows the arrangement for resolution testing, using a cod-liver oil capsule and a microfabricated phantom to show range and resolution. Imaging was carried out using a fast recovery fast spin echo sequence, with a transmit time (TR) of 33 ms and an echo time (TE) of 15 ms. Images were acquired as 28 slices of 1.2 mm

thickness, with 192 x 160 pixels per slice in an 80 mm x 40 mm field of view (FOV). The number of excitations (NEX) was 4, and the acquisition time was 5 min 42 sec. The sagittal image shown demonstrates a resolution of at least 1 mm. Tissue imaging was carried out using porcine liver, in the arrangement of Fig 15. A T_2-enhanced gradient echo sequence was used, with time constants TR = 33 ms and TE = 15 ms. Images were acquired as 28 slices of 1.2 mm thickness, with 256 x 256 pixels per slice in an 110 mm x 110 mm FOV and with NEX = 4. The acquisition time was again 5 min 40 secs. The axial slice image shows the top surface of the liver, together with evenly spaced portal tracts.

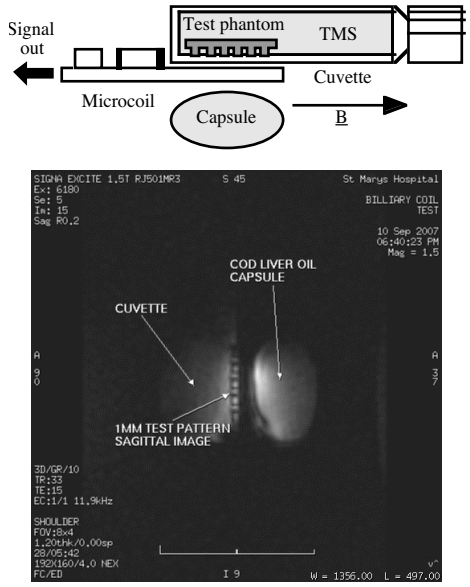

Figure 14. Arrangement for and result of resolution test.

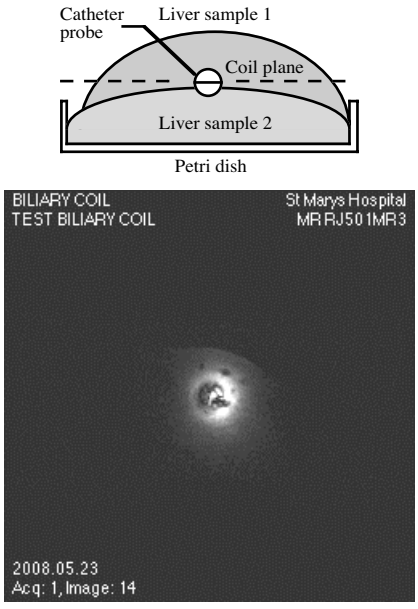

Figure 15. Arrangement for and result of tissue imaging.

VII CONCLUSIONS

Flexible rectangular spiral microcoils have been formed using planar processing on temporary carrier wafers from electroplated conductors on SU-8 substrates. Resonant microcoil detectors have been integrated into a catheter probe for biliary imaging. ^{1}H MRI experiments in a 1.5 T magnetic field show useful image resolution. Further work is in progress to improve microcoil reliability and to develop a non-magnetic endoscope for coil delivery into the bile duct.

REFERENCES

[1] Khan S.A., Thomas H.C., Davidson B.R., Taylor-Robinson S.D. "Cholangiocarcinoma" Lancet 366, 1303-1314 (2005)

[2] Vennes J.A., Jaconson J.R., Silvis S.E. "Endoscopic cholangiography in the diagnosis of obstructive jaundice" Gastroenterology 64, A132/815 (1973)

[3] Foutch P.G., Kerr D.M., Harlan J.R., Manne R.K., Kummet T.D., Sanowski R.A. "Endoscopic retrograde wire-guided brush cytology for diagnosis of patients with malignant obstruction of the bile duct" Am. J. Gastroenterology 85, 791-795 (1990)

[4] Arepally A., Georgiades C., Hofmann L.V., Choti M., Thuluvath P., Bluemke D.A. "Hilar cholangiocarcinoma: staging with intrabiliary MRI" Am. J. Roentgenol. 183, 1071-1074 (2004)

[5] Peck T.L., Magin R.L., Kruse J., Feng M. "NMR microspectroscopy on 100-μm planar RF coils fabricated on gallium arsenide substrates" IEEE T. Biomed. Eng. 41, 706-709 (1994)

[6] Neagu C.R., Jansen H.V., Smith A., Gardeniers J.G.E., Elwenspoek M.C. "Characterization of a planar microcoil for implantable microsystems" Sensors and Actuators A62, 599-611 (1997)

[7] Dechow J., Forchel A., Lanz T., Haase A. "Fabrication of NMR-microsensors for nanoliter sample volumes" Microelectr. Engng. 53, 517-519 (2000)

[8] Woytaskik M., Ginefri J.-C., Raynaud J.-S., Poirier-Wuinot M., Dufour-Gergam E., Grandchamp J.-P., Girard O., Robert P., Gilles J.-P., Martincic E., Darasse L. "Characterisation of flexible RF microcoils dedicated to local MRI" Microsyst. Technol. 13, 1575-1580 (2007)

[9] Ahmad M.M., Casperz W., Young I.R., Taylor-Robinson S., Syms R.R.A., Gedroyc W. "Flexible microcoils for in-vivo biliary imaging" Proc. ISMRM '08, Toronto, Canada, 3-9 May, p 441 (2008)

[10] Lorenz H., Despont M., Fahrni N., LaBianca N., Renaud P., Vettinger P. "SU-8: a low-cost negative resist for MEMS" J. Micromech. Microeng. 7, 121-124 (1997)